Development and Calibration of an Impulse Magnetic Field Measurement System for Lightning Electromagnetic Pulse Investigation

XIAO-MING REN, ZHENG-CAI FU, WEI SUN
Department of Electrical Engineering
Shanghai Jiao Tong University
No. 1954 Huashan Road, Shanghai
CHINA
rxm_213@163.com

Abstract: - In order to evaluate the impulse magnetic field distribution inside buildings truck by lightning or by nearby stokes, a set of measuring system composed of self-made magnetic detection coil and fiber transmission system was developed. The sensitivity coefficient of the optical fiber transmission system was calibrated by sine wave generator. Connecting the output of a portable 8/20μs current generator with a circular coil whose diameter is 0.3 m to compose the magnetic field generator, the detection coil was fixed in the center of the circular coil for calibration. The B/V calibrated coefficient error of the system is less than 3%. A demonstrating application of the developed measurement system is in the investigation of the electromagnetic environment in buildings under direct and nearby lightning strokes. Experimental verification of such application has been carried out on metal frame structure models of building in laboratory. Two scaled metal frame structure models are set up in the laboratory. The measured transient magnetic field distributions inside the building frame structures are verified by comparison of the testing results with the calculated results using the circuit method simulation. In the circuit method, the lightning channel and the building's metal cage are modeled by a multi-conductor system. Every branch conductor is divided into several suitable segments. The length of each segment is less than one tenth of the wavelength corresponding to the maximum frequency in the equivalent spectrum of the lightning transient current. Each segment is modeled by a coupled π-type lumped circuit. The test results of the developed measurement system coincide with the calculated results well. Under the situation of nearby lightning strokes, the developed measurement system is also used for the investigation of the shielding effectiveness of the building frame structure. The test results of the shielding effectiveness on the metal frame structure model shows that the effectiveness coefficient increases with the decrease of grid width of the frame. While the width of the grid changes from 0.5m to 0.25m, there is an increase of shielding effectiveness of approximately 10.2%. While the width of grid changes from 0.25 m to 0.125 m, the shielding effectiveness increases about 5%. To simulate the situation when metal plate wall exists in the building, 0.5 mm steel plate was attached on the frame structure model. Under such situation, the shielding effectiveness increases to 4.9. The application experiments of the developed measurement system show that it can fulfill the requirements of lightning impulse magnetic field measurement.

Key-Words: - impulse magnetic field, calibration, magnetic field generator, magnetic field measurement, lightning protection, fiber transmission system

1 Introduction

The damage to the information equipment caused by impulse magnetic field inside buildings struck by lightning or neighboring lightning strokes is increasing because of the wide application of information technologies. In order to evaluate the risk of damage, the detection technology of magnetic field under lightning situations needs to be investigated.

The transient magnetic field measurement technology has been applied mainly in two fields.

One is in the field of nuclear electromagnetic pulse (EMP) [1, 2, 3, 4, 5]. Another is in the field of pulse power generators where large impulsive voltages and currents and associated magnetic fields exist [6, 7]. ZHANG et al. adopted a single-turn coil of 80 mm radius as the magnetic field measurement probe, the dynamic measuring range of which ranged from $1 \sim 700$ A / m and the bandwidth is 40 Hz~100 MHz [8]. XIAO et al. designed a shielded ring magnetic probe with a radius of 2.5 cm, and its dynamic measuring range is $0.005 \sim 50$ A/m [9].

Since the magnetic field generated by lightning current can't be measured by the two systems mentioned above due to their relatively narrow measurement range, a set of measuring system composed of self-made multi-turn magnetic field detection coil and fiber transmission system was developed. The design of the multi-turn coil can increase the measurement range. The use of fiber transmission system can improve the anti-jamming capability.

2 Composition of the impulse magnetic field measurement system

The impulse magnetic field measurement system consists of the detection coil, the attenuator, the optical fiber transmission system, and an oscilloscope, as shown in Fig.1. The cross-section of the self-made coil is small, the shape of the coil is cylindrical, and its length is short. The magnetic field value measured by the detection coil transmits through the attenuator to the optical transmitter. The optical transmitter output signal is transmitted to the optical receiver via a multi-mode optical fiber. Finally the output signal of the optical receiver is transmitted to the oscilloscope Tektronix 3032B. In order to avoid signal distortion in a certain range of output values during transmission, the attenuator is adopted. To ensure accurate test results, the sensitivity coefficient of the detection coil and the coefficient of optical fiber transmission system need to be calibrated.
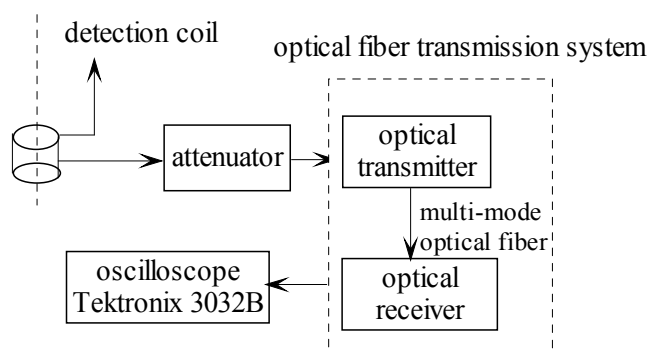
Fig.1 Composition of the impulse magnetic field measurement system

3 Sensitivity calibration of the optical fiber transmission system

Because the signal transmission path is in a strong electromagnetic environment, cables can not be adopted directly. Because of some characteristics such as wide broadband and strong resistance to

electromagnetic interference performance, optical fiber is ideal to be adopted as transmission signal path. The AlGaAs semiconductor with the light wavelength of 820nm is adopted as the light-emitting device [10, 11].

Fig.2 shows the insertion loss curve of optical fiber system which is measured by Agilent-4396B network analyzer. It can be seen from the curve that signal attenuation is less than 1dB and the transfer function curve has no significant mutations when the frequency is within the range of 100 kHz ~ 100 MHz. Because the lowest measurable frequency of Agilent-4396B is 100 kHz, the following response lower than this frequency is not shown in the figure. Table 1 is the test data of insertion loss. Tektronix AFG3021 can be used directly to finish the test of actual low-frequency limit. Test results show that the actual low-frequency limit can reach as low as 100 Hz. So the frequency bandwidth of the transmission system is 100 Hz ~ 100 MHz.
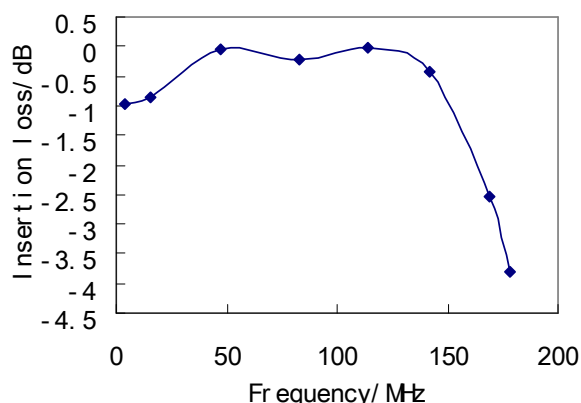
Fig.2 Insertion loss curve of the optical fiber transmission system

Table 1 Insertion loss test results

Number	Frequency (MHz)	Insertion loss (dB)
0	3.99	-0.96
1	15.49	-0.85
2	47.17	-0.04
3	83.15	-0.23
4	113.89	-0.02
5	142.13	-0.43
6	169.21	-2.54
7	178.46	-3.81

Fig.3 is the spectrum distribution of 12kA 8/20μs impulse current. Fig.3 shows that the amplitude is almost zero when frequency in above 400 kHz. The

upper frequency range of a lightning current need to be considered is about 1 MHz according to IEC 62305. Therefore the bandwidth can meet the requirements of the impulse magnetic field signal transmission.
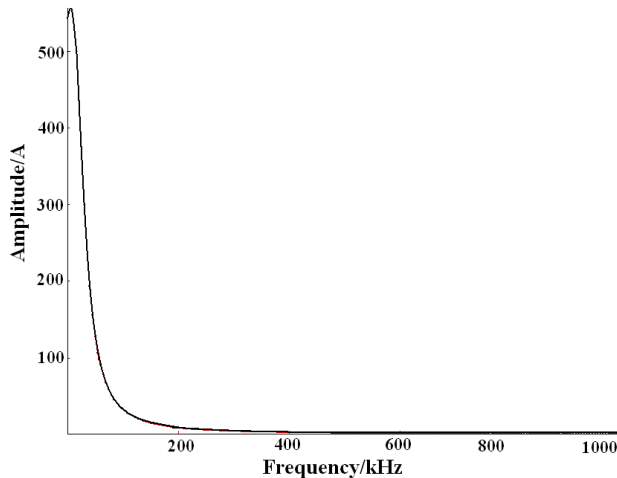
Fig.3 Spectrum of 12kA 8/20μs impulse current

The sensitivity coefficient of the optical fiber transmission system is calibrated by Tektronix AFG3021 signal source. The generator's frequency range is 1 Hz ~ 25 MHz and the accuracy is 1%.

In general, frequency of the transient magnetic field is within 1MHz, so the transmission coefficient of the transmission system can be calibrated by waveform amplitude changing at a fixed frequency. Sine-wave signal is selected because its peak voltage can easily be measured.

Sine-wave signal is input to optical fiber transmission system, and then output to the oscilloscope. The transmission coefficient is defined as the ratio of the output peak voltage to the input peak voltage.

The calibration test results of the optical fiber transmission system when the generator's frequency is 1MHz are shown in Table 2. Through the use of attenuator, the output peak voltage is within ± 1V. Calibrated average transmission coefficient is 13.28. The linearity error is less than 3%.

Table 2 Calibration test results of the optical fiber transmission system

Input peak voltage (V)	Output peak voltage (V)	Transmission coefficient	Relative error%
0.08	1.042	13.03	-1.9%
0.07	0.920	13.14	-1.0%
0.06	0.792	13.20	-0.6%
0.05	0.664	13.28	0.0%
0.04	0.534	13.35	0.6%
0.03	0.410	13.67	2.9%
0.02	0.268	13.40	0.9%
0.01	0.131	13.10	-1.3%
0.005	0.068	13.60	2.4%
0.002	0.026	13.00	-2.1%

4 The calibration of the detecting coil

4.1 The parameters of the detection coil

When the cylindrical detection coil, whose turns is N and the cross-sectional area is S, is put in the magnetic field of induction intensity B. The cross-section of the coil is made perpendicular to the magnetic field direction. The induced electromotive force generated in the coil is:

$$e(t) = -N \frac{d\phi}{dt} = -NS \frac{dB(t)}{dt} \qquad (1)$$

Where $NS = \frac{\pi}{12} N(D_1{}^2 + D_1 D_2 + D_2{}^2)$, which is called the coil constant [12]. Integration of the output signal of the detecting coil is needed when voltage signal $e(t)$ is reverted to the magnetic field signal. The self-inductance self-integral method is adopted with equivalent circuit shown in Fig.4. In Fig.4, $e(t)$ is the induction electromotive force, R is the coil resistance, L is the coil inductance, and R_1 is the measurement resistance.

The output voltage of the detecting coil can be expressed as

$$e(t) = L \frac{di(t)}{dt} + (R_0 + R_1)i(t) \qquad (2)$$

When $L \frac{di(t)}{dt} >> (R_0 + R_1)i(t)$, Equation (2) can be turned into
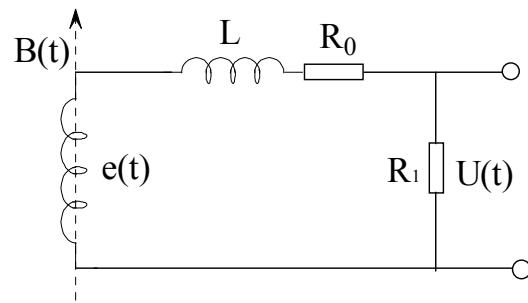
Fig.4 Equivalent circuit of the self-inductance self-integral method

$$e(t) \approx L \frac{di(t)}{dt} \qquad (3)$$

It can be obtained through alliance equation (1) and (3) that

$$- NS \frac{dB(t)}{dt} = L \frac{di(t)}{dt} \qquad (4)$$

$$i(t) = - \frac{NS}{L} B(t) \qquad (5)$$

Also, because

$$U(t) = R_1 i(t) = - \frac{NSR_1}{L} B(t) \qquad (6)$$

The measured magnetic induction intensity can be calculated as

$$B(t) = - \frac{L}{NSR_1} U(t) \qquad (7)$$

For the magnetic field detecting coil made based on the principle of electromagnetic induction for the measurement of non-uniform transient magnetic field, two requirements are needed.

1) The magnetic field detection coil should be as small as possible, which makes the magnetic field in the enclosed area could be approximately regarded as uniform, and the measurement results can approximately reflect the point magnetic field values along the coil center axis.

2) The presence of the coil should not have a significant impact to the magnetic field at the measurement point.

Therefore, the coil should be designed to become a "point" coil. However, because of its winding complex process, it can be replaced by cylindrical probe coil made according to a certain geometric design as shown in Fig.5. In the figure, the outer diameter D1 of the coil is 14.71 mm, the inner diameter D2 is 42.4 mm. Non-ferromagnetic materials is used for the I-shaped skeleton of the coil. The coil is made of 1200 turns.

Since this probe is used in the transient magnetic field measurement, so the inductance and resistance of the calculation formula should be changed with frequency changes. Since it is difficult to obtain a fix parameter via measurement according to equation (7), the best way is to calibrate the whole measurement system to obtain the B/V.
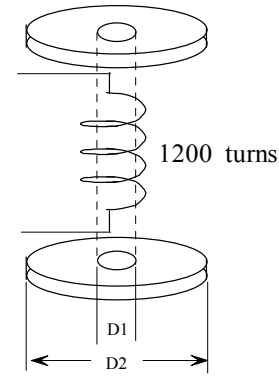
Fig.5 Schematic of the magnetic detecting coil

4.2 Calibration of the magnetic field detecting probe

According to IEEE standard 1309-1996, there are two ways for the calibration of the magnetic field detecting probe in the time domain [13]. 1) Compare the magnetic field probe which has been calibrated with the probe which needs to be calibrated. 2) Measure the magnetic field probe need to be calibrated in the reference magnetic field and then compare the measured magnetic field value with the calculated value.

The second method is adopted. The calibration system is shown in Fig.6. The Pearson Rogowski coil of type 5008C, whose sensitivity is 0.01 V / A, is adopted for the impulse current measurement.

The calculated magnetic field at the center point of the single-turn coil is

$$B = \frac{\mu_0 I}{2R} \qquad (8)$$

Where $\mu_0 = 4\pi * 10^{-7}$ H/m, R=0.15 m. The ratio between calculated magnetic field values and the measured probe coil voltage value B/V is called the coil sensitivity coefficient. Test data are shown in Table 3, where V_c is the measured magnetic field by the oscilloscope, V_T is the measured value of detection coil when transmission coefficient is 13.28 and the attenuation factor is 100. V_T can be calculated by equation (9).

$$V_T = \frac{V_c * 100}{13.28} = \frac{V_c}{0.1328} \qquad (9)$$

The linearity error of B/V is less than 3%, as shown in Fig.7. The measurement range of the

detection coil within the linear range is 0.25~1.94 mT, which is equivalent to about 200~1540 A/m.
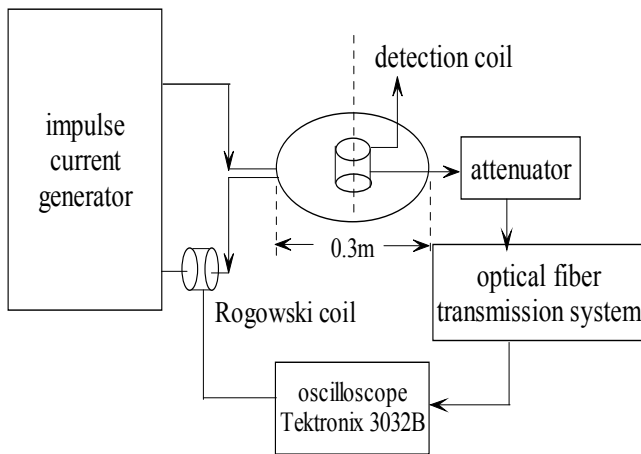
Fig.6 The detecting coil calibration system

If the attenuator factor is 10 and the transmission coefficient of optical fiber transmission system is 0.26, then the measurement range can be 0.79~9.79 mT, which is equivalent to 630~7770 A/m.

Fig.8 is measured magnetic field waveform when the impulse current is 60 A. Its timescale is 10 µs. Channel 1 is the impulse current waveform. Channel 2 is the magnetic field waveform measured by the probe coil. Through the combination of the attenuators and the optical fiber transmission system, its measurement range can reach 200~7770 A/m, and can meet measurement requirements of transient magnetic field. The magnetic field waveform and current waveform are almost the same at the rising edge, but some low-frequency distortion at the falling edge can be seen in the magnetic field waveform. This part of the distortion is caused by the bandwidth of optical fiber transmission system, because actual low-frequency limit is 100 Hz.

Table 3 Calibration data of the detecting coil

V_c (V)	V_T (V)	I (A)	B (mT)	B/V	error%
0.87	6.55	464	1.94	0.296	2.4%
0.81	6.09	424	1.78	0.291	0.5%
0.74	5.57	380	1.59	0.285	-1.4%
0.65	4.89	336	1.41	0.287	-0.8%
0.54	4.07	280	1.17	0.288	-0.5%
0.5	3.76	260	1.09	0.289	-0.2%
0.44	3.31	226	0.95	0.285	-1.4%
0.38	2.83	194	0.81	0.286	-1.0%
0.32	2.38	164	0.69	0.288	-0.4%
0.23	1.75	120	0.50	0.287	-0.7%
0.17	1.29	92	0.38	0.297	2.7%
0.11	0.86	60	0.25	0.292	1.0%
coefficient B/V average value				0.289	

The relationship between the voltage signal $U_0(V)$ measured by the oscilloscope and the real value of magnetic field $B(T)$ is as following:

$$B = 0.21 \times 10^{-4} U_0 \qquad (10)$$
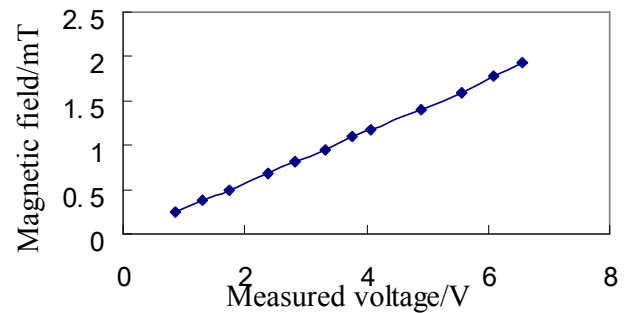
Fig.7 Linearity test result of B/V
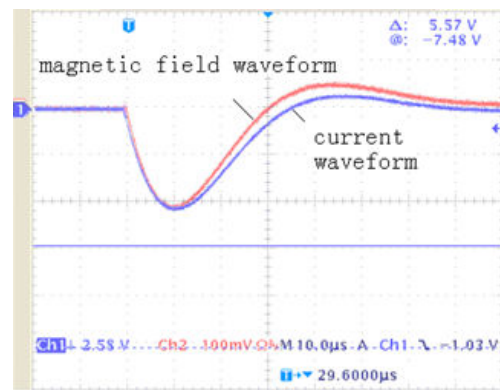
Fig.8 Measured magnetic field waveform

5 Application of the developed measurement system

A typical building lightning protection system (LPS) includes the air-terminal system, down-conductor system and grounding grid. In most of the cases, the entire metal frame structure which is embedded in the inner part of the building is employed as the down-conductor. In other cases, the down conductor may also be independent down-conductor structure which is laid on the outside of the building and is insulated from the inner metal frame structure of the buildings.

The distribution of magnetic field in the building is induced by transient current distributed along the independent down-conductor and the induced transient current on the inner metal structures.

Through the mutual interaction of inductance and capacitance between down-conductor and the metal structures of the building, induced current is generated on the metal structures inside the building though inductive coupling of the magnetic field and capacitive coupling of the electric field.

The down-conductor system could be separated into several segments which can be expressed by π-type lumped parameter equivalent circuit. Fig.9 shows the coupling relationship between one segment of the external lightning protection down-conductor and the metal framework of the building. L_s and R_s are the inductance and the resistance of one segment of down-conductor respectively. C_{s1} and C_{s2} are ground capacitance respectively. L_m, C_{m1} and C_{m2} are mutual inductance and mutual capacitance between one segment of the down-conductor and the metal framework of the building.

The coupling effect between different branches should be considered in calculating induced current distribution when the metal framework of the building is stuck by nearby lightning strikes, because the induced current is generated by the action of electromagnetic coupling between the main discharge channel and the metal framework.
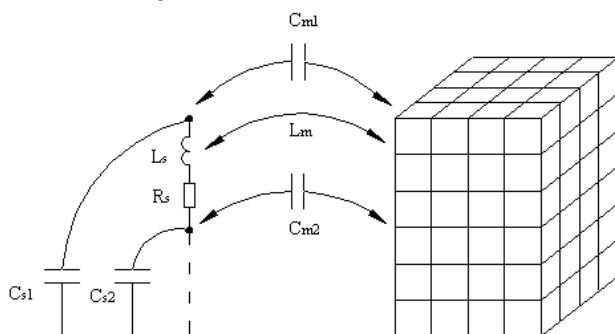
Fig.9 Inductive coupling and capacitive coupling of nearby lightning strikes

The circuit method is adopted in numerical calculation. Lightning current is represented by the traditional double exponential waveform. The metal framework and the independent down-conductor are expressed with equivalent branch of conductors. All the branches of conductors need to be divided into appropriate segments, the length of each segment can not exceed one-tenth of the wavelength corresponding to the maximum frequency component of the lightning current.

Due to the frequency-dependent parameters which include resistance of the structure, self-inductance, self-capacitance of different sections and the mutual inductance, the mutual capacitance, and mirror effect of the earth, every section can be simulated by coupling π-type lumped parameter equivalent circuit.

Among them, self-inductance and mutual inductance can be calculated using the Neumann integral formula which has considered the depth of penetration of earth effect. Self-capacitance and mutual capacitance can be calculated using the average potential method. The lightning current waveform described by double-exponential function can be Fourier transformed (FFT).

The current distribution and node voltages of different branches in the frequency domain can be obtained by solving the circuit matrix equation under the corresponding frequency. The computation formula is as follows:

$$\begin{bmatrix} A & Y \\ Z & G \end{bmatrix} \begin{bmatrix} \dot{I}_b \\ \dot{V}_s \end{bmatrix} = \begin{bmatrix} \dot{I}_s \\ 0 \end{bmatrix} \qquad (11)$$

Where, A —— node correlation matrix

Y —— node admittance matrix

Z —— complex impedance matrix

G —— voltage coefficient matrix

I_b、V_s —— current vector and node voltage vector of branch

Then the transient current distribution of different branches in time domain can be obtained through the inverse Fourier transform (IFFT). When the current distribution of the metal framework is known, the magnetic field distribution inside building can be obtained using the Maxwell equations and the Biot-Savart law.
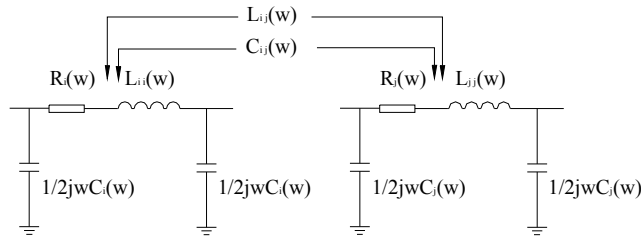
Fig.10 Coupled π-type lumped parameter circuit

In order to verify the applicability of the developed measurement system, scale models of metal framework had been erected in the laboratory. The magnetic field distribution can be measured by the developed magnetic field measurement system.

5.1 Experimental verification under situations of direct lightning strokes

The scale model of building has been erected in the laboratory as shown in Fig.11. The model adopted round steel with the diameter of 1 cm and the length

of 0.5 m as material to constitute 3×4×3 conductor

grid. 7.8/16μs test current whose peak value is 1.7 kA is imposed on the model. The Pearson Rogowski coil is adopted for the impulse current measurement and the magnetic field measurement system is used to measure magnetic field.
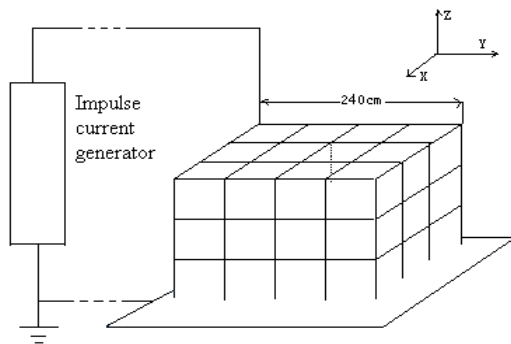
Fig.11 The scale model of the metal framework under direct lightning strokes
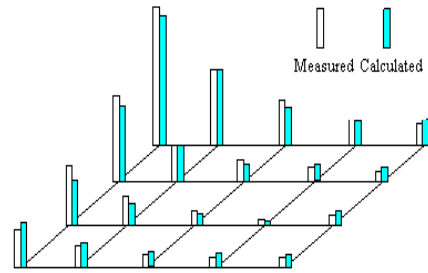
Fig.12 The measured and calculated value of branch conductor's diverter coefficient
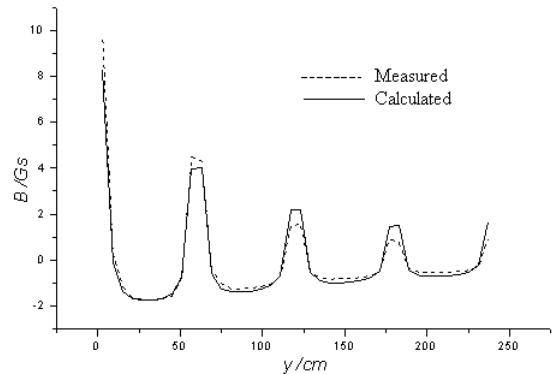
Fig.13 The comparison between magnetic field measurement and calculated results

The simulation results can be obtained by using corresponding pulse current waveform parameters in the simulation procedure. Measured and calculated values of the diverter coefficient of the vertical branch in the second floor are shown in Fig.12. The diverter coefficient is defined as the ratio of current peak flowing through a branch to the total injection current peak. The results show that the measured and calculated current distribution are consistent, the discrepancy between them is less than 10%.

In order to minimize the effect of lead line on space magnetic field, the test current is introduced from the Y-axis direction, and then the results of measured and simulated magnetic field of the Y direction can be compared. Fig.13 shows the measured and calculated magnetic induction intensity of various points which lie in Z = 90 cm (second layer), X = 3 cm, the measured values and calculated values are consistent.

5.2 Experimental verification under situations of nearby lightning strokes

In order to investigate the induced currents on the metal framework and its internal magnetic field distribution when under the situation of nearby lightning strikes, the metal framework and the scale

model of external lightning protection down-conductor have been erected in the laboratory, as shown in Fig.14.
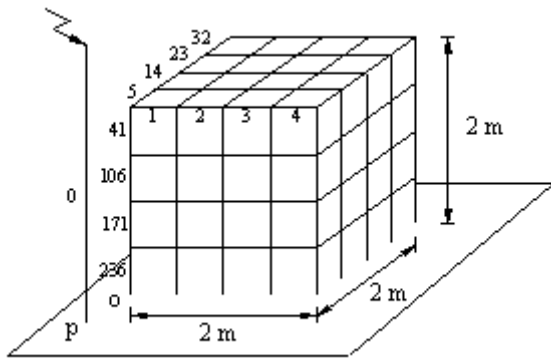
Fig.14 The scale model of the metal
framework under the situation of nearby
lightning strokes

The model is welded by 260 round steel conductor whose diameter and length is 1 cm and 0.5 m respectively. In all directions of length, width and height, the building conducting structure model are all divided into 4 uniform sections to simulate a complex three-dimensional metal grid structure. External lightning protection down-conductor is simulated with the round steel whose height and diameter is 2.5 m and 1 cm respectively. The metal framework is located in the center of a square iron plate; while the down-conductor is located in the diagonal line of the square iron plate. The distance between the down-conductor and the nearest vertical round steel is 1.414 m.

The surge current is applied to the external independent down-conductor from an impulse current generator. The thickness, width and length of the connecting copper belt is 0.6 mm, 9.8 cm and 3.2 m respectively. Point o is set as the coordinate origin. The conductivity of the round steel is 9.78×10^{-6} S/m, and the grounding resistance is $0.5\,\Omega$.

According to the model structure shown in Fig.14 and related parameters, numerical calculation circuit model can be established. The applied impulse current can be expressed as:

$$i(t) = I_0(e^{-\alpha t} - e^{-\beta t}) \quad (12)$$

Corresponding to the applied 7.4/18.2μs impulse current whose peak value is 5kA in the experiment, the calculated parameters are $I_0 = $ 161kA, $\alpha = $ 0.128257, and $\beta = $ 0.139532. The effect of

imbalances distribution of current caused by copper lead line has been taken into account.

At the measuring height of 0.75 m, the magnetic field peak value of 24 equally distributed points on the diagonal line in the framework have been measured in the experiment. The distribution of measured points is shown in Fig.15.
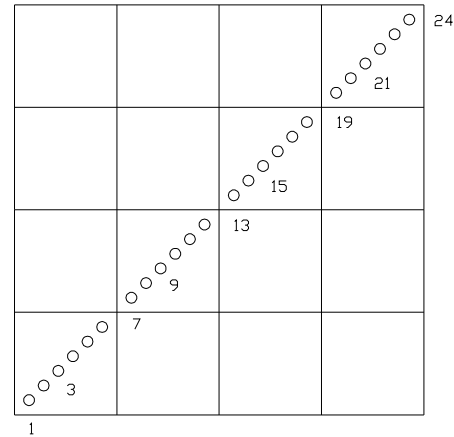
Fig.15 The distribution of the measured and

calculated points (top view)

Because of the dispersion of discharge, the distribution of magnetic field are represented with B/I(Gs/kA), where B is the magnetic induction intensity of each measured points, I is the peak current flowing through the down-conductor. In order to reduce the effect of the main discharge circuit on the measurement, only the magnetic field along the Y direction has been measured. Fig.16 shows the comparison results of the measured values and calculated values of the measured points.

Fig.16 shows that the calculation results coincide with experimental results. In the middle part of the building model, due to the small magnetic field and the difficulty of positioning the detection coil, there is a relatively large measurement deviation.
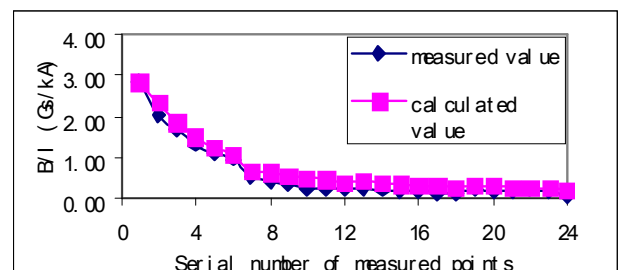
Fig.16 The comparison of the measured values and
calculated values of inner magnetic field distribution

5.3 Shielding effectiveness test of metal frame structure under nearby lightning strokes

One side of the metal frame is divided into four parts with a grid size of 0.5 m as the black bold lines shown in Fig.17. Since the magnetic flux density on the axial line is the principal concern, the frame which is vertical to the axial line is divided. In order to insure the same size of the grid, the grid can be further divided into 16 and 64 parts, with grid size of 0.25 m and 0.125 m respectively. Their shielding effectiveness under the conditions mentioned above can be measured.
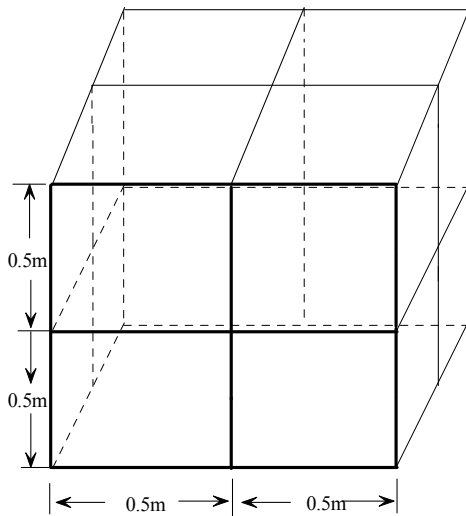
Fig.17 Configuration of the building frame

Shielding effectiveness testing system is shown in Fig.18. The distance d1 between the center of detection coil and magnetic field generator center is set as 1m, the distance d2 between the magnetic field generator center and the frame is set as 0.8 m. Without grid frame, while the generator output current is 570 A, U_0 is 0.376 V, according to formula (10), B_0 is 7.89 µT.

Because the center of detection coil and coil of magnetic generator are on the same axial line, therefore formula (8) can also be used to calculate the value of B, and the result is 7.79 µT, with the error of 1.3% when compared with the measured value.
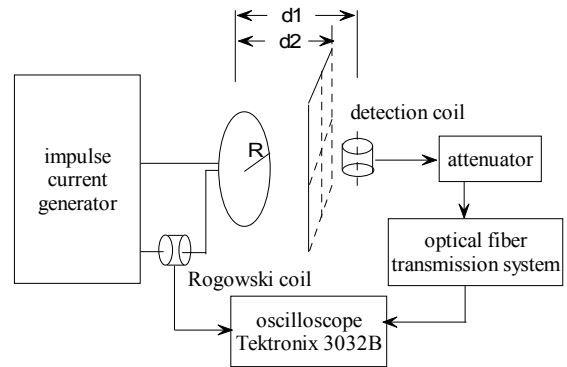
Fig.18 The shielding effectiveness testing system

The effectiveness of the electromagnetic shielding can be represented using the ratio between the magnetic field B_0 without the shielding and B with the shielding [14], therefore

$$\eta = \frac{B_0}{B} \qquad (13)$$

$$S_E = 20 \bullet \lg \eta \qquad (14)$$

The detailed test results are shown in Table 4, where w is grid width and V_1 is the measured value of measurement system. While the width of the grid changes from 0.5 m to 0.25 m, there is a change of η approximately 10.2%. While the width of the grid changes from 0.25 m to 0.125 m, the change of η is about 5%, which indicates that with the decrease of grid width, the change of η slow down. When the 0.5 mm steel plate was used, the value of η is 4.9.

Table 4 Shielding effectiveness under various grid width and metal plate

Number of grid	w (m)	V_1 (V)	B (µT)	η	S_E (dB)
4	0.500	0.296	6.21	1.27	2.07
16	0.250	0.268	5.62	1.40	2.92
64	0.125	0.256	5.37	1.47	3.35
steel plate	/	0.077	1.61	4.90	13.80

6 Conclusions

The measurement range of the developed impulse magnetic field measurement system can reach 200～7770A/m. The frequency bandwidth of the transmission system is 100 Hz～100 MHz. The linearity calibration error of the system is less than 3%. In addition, the application of the optical fiber

transmission system can increase the anti-jamming capability of the measurement system. The developed system can meet the measurement requirements of transient magnetic field.

The tests under direct and nearby lightning strike situations using the developed measurement system have been carried out to verify the applicability of the system. The test results show that the calculation results coincide with experimental results. The test of shielding effectiveness of the building metal frames also shows that the system is applicable for the test of transient magnetic field.

The applications of the developed system show that it is applicable in the investigation of lightning electromagnetic environments.

References:

[1] Carl E. Baum, E.L. Breen, F.L. Pitts, G.D. Sower, and M.E. Thomas, The Measurement of Lightning Environmental Parameters Related to Interaction with Electronic Systems, *IEEE TRANSATIONS ON EMC*, Vol.44, No.2, 1982, pp.123-137

[2] Carl E. Baum, Moto Kanda and Carl on Electromagnetic Sensors, *IEEE TRANSATIONS ON EMC,* Vol.44, No.1, 2002, pp. 16-17

[3] Miguel A. Fuentes, Adnan Trakic, Analysis and Measurements of Magnetic Field Exposures for Healthcare Workers in Selected MR Environments, *IEEE TRANSACTIONS ON BIOMEDICAL ENGINEERING*, Vol.55, No.4, 2008, pp.1355~1364

[4] James Lenz and Alan S. Edelstein, Magnetic Sensors and Their Applications. *IEEE SENSORS JOURNAL*, Vol.6, No.3, 2006 , pp. 631~649

[5] R. Grössinger, M. Taraba, and A. Wimmer. Calibration of an Industrial Pulsed Field Magnetometer, *IEEE Transactions on magnetics*, Vol.38, No.5, 2002 , pp. 2982~2984

[6] C.Ramachandran, P.David, Wang Kai, Characterization of human metal ESD reference discharge event and correlation of generator parameters to failure levels-part I: reference event, *IEEE Transactions on Electromagnetic Compatibility*, Vol.46, No.4: 2004, pp. 498-504.

[7] M. Kanda, Standard probes for electromagnetic field measurement, *IEEE TRANSACTIONS ON ANTENNAS AND PROPAGATION*, Vol.41, No.10, pp.1349-1364

[8] ZHANG Wei-dong, CUI Xiang, Development of an Optical Fiber Transient Magnetic Field Sensor and Its Application . *Proceedings of the CSEE(in Chinese)*,Vol.23, No.1, 2003, pp. 88-92

[9] XIAO Baoming, WANG Zezhong, LU Binxian, LI Yunwei, Research of Measurement System of Transient Weak Magnetic Field. *High Voltage Engineering(in Chinese)*, Vol.31, No.1, 2005, pp. 53-54

[10] LIU Jun, XU Yan, Design and Simulation of High Pulse Magnetic Field Measurement System, *Electrical Measurement & Instrumentation(in Chinese)*, Vol. 43, No.9, 2006 , pp. 11-14

[11] LI Yanxin, SHI Lihua, ZHOU Bihua, Measurement of Pulse Electromagnetic Field Using Wide Band Fiber Optic Analogue Transmission System, *High Voltage Engineering(in Chinese)*, Vol. 32, No.2, 2006, pp. 34-36

[12] Li Daming, *Measurement of magnetic field*, China Machine Press, 1993

[13] IEEE Std 1309-1996, IEEE Standard for Calibration of Electromagnetic Field Sensors and Probes, Excluding Antennas, from 9kHz to 40GHz, The IEEE, 1996

[14] Gao Cheng, Chen Bin, Zhou Bihua. Portable magnetic Shielding Effectiveness Measurement Device, *High Voltage Engineering(in Chinese)*, Vol.28, No.6, 2002, pp.27-29

Xiaoming Ren was born in Zhejiang, China on September, 10 1977. He received his B. Sc degree in 2000 from Jianghan Petroleum institute and M. Sc degree in 2004 from Wuhan University of technology. He is currently pursuing his Ph.D degree at Shanghai Jiao Tong University. His research interests are lightning protection and EMC.

Zhengcai Fu was born in Zhejiang, China, in 1965. He received the B.Sc., M.Sc. and Ph.D. degrees in electrical engineering from Shanghai Jiao Tong University, Shanghai, China, in 1987, 1990 and 2001, respectively. He is currently a professor in the Department of Electrical Engineering, Shanghai Jiao Tong University, Shanghai, China. His research

interests are over voltage and insulation coordination, high voltage test technique and EMC.

Wei Sun was born in Shanghai, China, in 1963. He received his B.Sc. and M.Sc. degree in electrical engineering from Shanghai Jiao Tong University, Shanghai, China, in 1985, 1989, respectively. He is currently a senior engineer in the High Voltage Laboratory of Shanghai Jiao Tong University, Shanghai, China. His research interests are high voltage test technique and EMC.